

This discussion paper is/has been under review for the journal Climate of the Past (CP).
Please refer to the corresponding final paper in CP if available.

Variability of summer humidity during the past 800 years on the eastern Tibetan Plateau inferred from $\delta^{18}\text{O}$ of tree-ring cellulose

J. Wernicke, J. Grießinger, P. Hochreuther, and A. Bräuning

Institute of Geography, Friedrich-Alexander-University, Erlangen-Nuremberg, Germany

Received: 2 July 2014 – Accepted: 28 July 2014 – Published: 15 August 2014

Correspondence to: J. Wernicke (jakob.wernicke@fau.de)

Published by Copernicus Publications on behalf of the European Geosciences Union.

Title Page

Abstract

Introduction

Conclusions

References

Tables

Figures



Back

Close

Full Screen / Esc

Printer-friendly Version

Interactive Discussion



Abstract

We present an 800 years long $\delta^{18}\text{O}$ chronology from the eastern part of the Tibetan Plateau (TP). The chronology dates back to 1193 AD and was sampled in 1996 AD from living *Juniperus tibetica* trees. The chronology is unique for eastern Tibet and provides a reliable archive for hydroclimatic reconstructions. Highly significant correlations were obtained with air moisture (relative humidity, vapour pressure and precipitation) during the summer season. We applied a linear transfer model to reconstruct the summer season relative humidity variation over the past 800 years. We identified more moist conditions at the termination of the Medieval Warm Period, an oscillating air humidity around the mean during the Little Ice Age and a sudden decrease of relative humidity since the 1870s. The late 19th century humidity decrease is in good accordance with several multiproxy hydroclimate reconstructions for south Tibet. On the other hand, since the end of the 19th century strong evidences for an increase in humidity on the northern TP is exhibited. Spatial correlation analysis with the North Atlantic Oscillation index (NAO) and the sea surface temperature (SST) of Niño region 3.4 reveal a weak and nonstationary relationship to the $\delta^{18}\text{O}$ chronology. Instead, spatial correlations expose a dominating convective influence to the relative humidity reconstruction. Furthermore, wavelength analysis reveal good agreements between the significant cyclicities in our $\delta^{18}\text{O}$ chronology and several moisture sensitive proxy archives.

1 Introduction

The variation in strength, timing and duration of the Asian summer monsoon (ASM) system affects life and economy of many millions of people living in south and east Asia (Vuille et al., 2005). In remote areas, such as the Tibetan Plateau (TP), reliable climate records are short and scattered. Nevertheless, a recent weakening trend of the ASM was reported in several studies (Bollasina et al., 2011; Sano et al., 2011;

CPD

10, 3327–3356, 2014

East Tibet hydroclimate variability

J. Wernicke et al.

Title Page

Abstract

Introduction

Conclusions

References

Tables

Figures



Back

Close

Full Screen / Esc

Printer-friendly Version

Interactive Discussion



East Tibet hydroclimate variability

J. Wernicke et al.

Title Page

Abstract

Introduction

Conclusions

References

Tables

Figures



Back

Close

Full Screen / Esc

Printer-friendly Version

Interactive Discussion



Zhou et al., 2008). The decline in air humidity was explained by the thermal gradient reduction between the surface temperatures of the Indian Ocean and the TP due to Global Warming (Sun et al., 2010). Contemporaneously, different locations and climate archives reveal a strengthened monsoonal precipitation (Anderson et al., 2002; Kumar et al., 1999; Zhang et al., 2008). This discrepancy may be explained by the high variability of the monsoon circulation itself, but also due to a limited number of available palaeoclimate studies and resulting climate modeling uncertainties. Thus, for a better understanding of the circulation system as a whole, but also for the verification of climate change scenarios, a keen demand for reliable climate reconstructions exists for the TP. With increasing numbers of palaeoclimatic records, forecast precision increases and therewith strong implements for decision makers can be achieved.

The dislocation of the Intertropical Convergence Zone (ITCZ) on the Northern Hemisphere in boreal summer is amplified over the Asian continent by the thermal contrast between the Indian Ocean and the TP. Convective rainfalls during the summer monsoon season between June and September are strongly altered by the complex topography of the Himalayas and western Chinese mountain systems (e.g. Böhner, 2006; Thomas and Herzfeld, 2004). Extreme climatic events that may have devastating effects, but also long-term trends of ASM intensity are therefore in the focus of numerous climate reconstruction efforts (e.g. Cook et al., 2010; Xu et al., 2006b; Yang et al., 2003). Most of these studies use tree-ring width as a proxy for palaeoclimate reconstructions. Nonetheless, several studies demonstrated that $\delta^{18}\text{O}$ of wood cellulose is a strong indicator of hydroclimatic conditions (McCarroll and Loader, 2004; Roden et al., 2000; Sauer et al., 1997; Sternberg, 2009). Even if tree stands were influenced by external disturbances (e.g. competition, insect attacks or geomorphological processes) they still reflect variations of the local hydroclimate accurately (Sano et al., 2013). Recently published tree-ring $\delta^{18}\text{O}$ chronologies from the TP show a common strong response to regional moisture changes. Grießinger et al. (2011) successfully reconstructed August precipitation over the past 800 years. They demonstrated reduced precipitation during the Medieval Warm Period (MWP), reinforced rainfalls during the

**East Tibet
hydroclimate
variability**

J. Wernicke et al.

[Title Page](#)[Abstract](#)[Introduction](#)[Conclusions](#)[References](#)[Tables](#)[Figures](#)[Back](#)[Close](#)[Full Screen / Esc](#)[Printer-friendly Version](#)[Interactive Discussion](#)

Little Ice Age (LIA) and decreasing precipitation rates since the 1810s. In addition, shorter $\delta^{18}\text{O}$ chronologies from the central Himalayas showed consistent negative correlations to summer precipitation (Sano et al., 2010, 2011, 2013). The detected recent reduction of monsoonal precipitation has been interpreted as a reaction to increased sea surface temperatures over the tropical Pacific and Indian Ocean. Strong responses to regional cloud cover changes were found for tree-ring $\delta^{18}\text{O}$ chronologies from the south-eastern TP (Liu et al., 2013, 2014; Shi et al., 2012). The local moisture reduction since the middle of the 19th century is less pronounced than for south-west Tibet and was associated with complex El Niño-Southern oscillation teleconnections (Liu et al., 2012). Existing tree-ring $\delta^{18}\text{O}$ chronologies on the north-eastern part of the plateau respond sensitive to local precipitation and relative humidity, although the relationships are inverse (Wang et al., 2013; Yu et al., 2008). Except for a relatively short summer moisture sensitive time series (An et al., 2014), no long-term $\delta^{18}\text{O}$ chronologies and reliable reconstruction have been conducted for the eastern TP so far. Therefore it still remains unclear if and to which extent the MWP, LIA and the modern humidity decrease are reflected in tree-ring $\delta^{18}\text{O}$ series in the transitional zone of the eastern TP, where the influence of the ASM, the Indian Summer monsoon and the westerlies overlap.

We present a newly developed, well replicated, 800 years long $\delta^{18}\text{O}$ chronology, representing a unique archive for studying the past hydroclimate in eastern Tibet. We applied response and transfer functions and obtained a reliable reconstruction of summer relative humidity (July and August). We compared the long-term trend of our chronology to other moisture sensitive proxy archives from several sites over the TP and discuss the influence of Pacific sea surface temperatures, the North Atlantic Oscillation (NAO) and local climate conditions on our $\delta^{18}\text{O}$ time series.

2 Material and methods

2.1 Study site – Lhamcoka

Lhamcoka is located on the eastern TP (see Fig. 1 green pentagon). During a field campaign in 1996, 16 increment cores of living *Juniperus tibetica* trees were taken. The samples were collected from a steep, south-east exposed slope at an elevation of 4350 m a.s.l. (31°49' N/99°06' E). The oldest tree ages up to 804 years, resulting in an overall chronology time span of 1193–1996 AD. Juniper builds the upper timberline in the region due to its cold temperature tolerance (Bräuning, 2001). The species' tree-ring growth is limited by temperature and spring precipitation (February–April) (Bräuning, 2006). Due to the steep slope angle of more than 30° and well drained substrate properties at the study site, ground water influence can be excluded. Therefore we assume that water absorption by trees is mainly triggered by summer precipitation.

Lhamcoka is influenced by the Indian Summer Monsoon system with typical maxima of temperature and precipitation during the summer months (see climate diagram in Fig. 1). The nearby climate station Derge (3201 m a.b.s.l., 50 km distance to sampling site) records 78% (541 mm) of its annual precipitation between June and September which is in accordance to common monsoonal climate properties (Böhner, 2006). The Derge climate record revealed increasing temperatures of about 0.6° C during the period 1956–1996, whereas the amount and interannual variability of precipitation remains constant within these 41 years.

Five trees were chosen for isotope analysis, to adequately capture inter-tree variability of $\delta^{18}\text{O}$ (Leavitt, 2010). The trees were selected according to (i) old age of the cores to extend the length of the derived reconstruction, (ii) avoidance of growth asymmetries due to slope processes, (iii) sufficient amounts of material (samples with wider rings were favoured), and (iv) a high inter-correlation among the tree-ring width series of the respective cores.

CPD

10, 3327–3356, 2014

East Tibet hydroclimate variability

J. Wernicke et al.

Title Page

Abstract

Introduction

Conclusions

References

Tables

Figures



Back

Close

Full Screen / Esc

Printer-friendly Version

Interactive Discussion



2.2 Sample preparation

We used the tree-ring width master chronology of Bräuning (2006) in order to date each annual ring precisely. The dated tree-rings were cut with a razor blade under a microscope. $\delta^{18}\text{O}$ values were measured from each tree individually in annual resolution.

5 Only at parts with extremely narrow rings, we obtained sufficient amounts of material by shifted block pooling (Böttger and Friedrich, 2009). Pooling was applied between the years 1864–1707 (see chronology parts with missing EPS in Fig. 2). To obtain pure α -cellulose, we followed the chemical treatment presented in Wieloch et al. (2011). The α -cellulose was homogenised with an ultrasonic unit and the freeze dried material was
10 loaded into silver capsules (Laumer et al., 2009). The ratio of $^{18}\text{O}/^{16}\text{O}$ was determined in a continuous flow mass spectrometer (Delta V Advantage; Thermo Fisher Scientific Inc.).

2.3 Statistical analyses

We used standard dendrochronology techniques of chronology building, model building and verification for the purpose of a reliable climate reconstruction (Cook and Kairiukstis, 1990). All analysis were conducted with the open source statistical software R (<http://cran.r-project.org/>). The stable isotope chronology was calculated within the “dplR” package developed by Bunn (2008) and the dendroclimatological correlation and response analyses were conducted by the “bootRes” package (Zang and Biondi,
20 2012). The pooling method we executed required a running mean calculation. Thus, the presented chronology has a quasi annual resolution, smoothed with a five years running mean filter. To evaluate the isotope chronology reliability the Expressed Population Signal (EPS, introduced by Wigley et al., 1984) and the Gleichläufigkeit (GLK) were computed. The EPS expresses the variance fraction of a chronology in comparison with a theoretically infinite tree population, whereas the GLK specifies the proportion of agreements/disagreements of interannual growth tendencies among the trees
25

Title Page

Abstract

Introduction

Conclusions

References

Tables

Figures



Back

Close

Full Screen / Esc

Printer-friendly Version

Interactive Discussion



3.2 Climatic response of tree-ring stable oxygen isotopes

We conducted linear correlation analyses between the $\delta^{18}\text{O}$ values and monthly climate data as well as calculated seasonal means of climate elements. The available climate record of station Derge covers 41 years (1956–1996 AD) and correlations were calculated for temperature (mean), precipitation, relative humidity, sunshine hours, and vapour pressure (see Fig. 3).

Summer moisture conditions explain most of the variance of the $\delta^{18}\text{O}$ chronology during the calibration period (1956–1996 AD). The stable oxygen isotopes are highly significantly ($p < 0.01$) correlated with precipitation, relative humidity, sunshine hours and vapour pressure during July and August. Highest (negative) correlations were obtained with relative humidity during July ($r = -0.73$) and July/August ($r = -0.71$). Thus, if relative humidity is high, evapotranspiration is lowered and the depletion of light ^{16}O due to leaf water fractionation is reduced. Bräuning (2006) has been demonstrated a positive impact of early summer temperatures for the tree-ring width growth. A similar relationship to the $\delta^{18}\text{O}$ signal is implied by a positive feedback with May temperatures. Sunshine hours were inversely correlated with the oxygen isotope values. An enrichment of heavy isotopes was observed if the number of sunshine hours are high and the cloud cover is low, respectively. Very weak correlations were found with climate conditions during the previous year. Therefore, plant physiological carry over effects as well as stagnating soil water can be regarded as inferior factors for tree-ring $\delta^{18}\text{O}$ variations. We found indications for colinearities between the specification of α -cellulose in July–August and relative humidity as well as with sunshine hours. The explained variance of linear regressions between stable oxygen isotopes and relative humidity accounts for 53% and for 33% for sunshine hours, respectively. Hence, the $\delta^{18}\text{O}$ value mainly depends on relative humidity, which is in accordance to findings of Roden and Ehleringer (2000). Although highest correlations were obtained with single months (July: $r = -0.71$ ($p < 0.01$)), the reconstruction was established for the summer season (mean relative humidity of July and August). In terms of using wood cellulose of

Title Page

Abstract

Introduction

Conclusions

References

Tables

Figures



Back

Close

Full Screen / Esc

Printer-friendly Version

Interactive Discussion



a single year, the humidity reconstruction of the major growing season is rather robust than of single months.

3.3 Reconstruction of relative humidity

We employed a linear model for the reconstruction of relative humidity over the past 800 years. The linear relationship was achieved for the $\delta^{18}\text{O}$ values and instrumental records of relative humidity at climate station Derge between 1956–1996 AD. The model was validated according to standard methods presented in Cook and Kairiukstis (1990) and Cook et al. (1994). We applied the leave-one-out validation procedure due to the short time period of available climate data. The model statistics are summarized in Table 1.

The validation tests indicated that (1) the number of agreements between the reconstructed climate series and the meteorological record is according to the sign orientation significantly different from a pure chance driven binominal test (ST); (2) the cross-correlation between the reconstruction and the measurement is highly significant (PMC, PMT) and (3) the reconstruction is reliable due to a positive RE and CE, indicating the reconstruction is better than the calibration period mean (Cook et al., 1994). Thus, our linear model is suitable for the climate reconstruction. The model related to the reconstruction of summer relative humidity is described as: $\text{RH}_{\text{JA}} = -2.3 \cdot \delta^{18}\text{O} + 125.3$ (RH_{JA} , expressed in %).

Our reconstruction reveals several phases of high and low summer humidity (see Fig. 4). Negative deviations from the mean value (72.4 %; $\text{sd} = 4.9\%$) occurred during 1300–1345, 1475–1525, 1630–1670 and 1866–1996 (periods are emphasized with dashed vertical lines in Fig. 4). The most pronounced relative humidity depression started in the late 1870s and lasts until the end of the reconstruction in 1996 (dashed red line in Fig. 4). The period is characterized by the driest summer in 1943 ($\text{RH} = 68.4\%$). The remarkable moisture reduction since the end of the LIA is confirmed for the southern and south-eastern part of the TP (Liu et al., 2014; Xu et al., 2012; Zhao and Moore, 2006). More humid periods were detected during 1193–1300, 1345–1390,

East Tibet hydroclimate variability

J. Wernicke et al.

Title Page

Abstract

Introduction

Conclusions

References

Tables

Figures



Back

Close

Full Screen / Esc

Printer-friendly Version

Interactive Discussion



ues of Lhamcoka ($r = -0.16$, $p < 0.01$). The snow accumulation rate of Dasuopu ice core has no relationship to our $\delta^{18}\text{O}$ chronology ($r = -0.04$, $p = 0.3$). In case of weak correlations and due to the degrees of freedom ($\text{DF} > 100$), significance levels alone might be misleading and indicate only a statistical and not a causal relationship. However, strong relationships between the tree-ring $\delta^{18}\text{O}$ chronologies of Lhamcoka and Ranwu, and partly Reting, are reasonable. In Fig. 4 we highlighted the MWP (yellow polygon), LIA (blue polygon), dry phases in east Tibet (dashed lines) and the remarkable humidity decline since the late 1870s (dashed red line). The MWP is characterized by more humid conditions on the eastern TP (Lhamcoka), a drier phase on the central plateau (Reting) and moderate moisture conditions on the northern plateau (Dulan). During the LIA a remarkable moisture increase occurred at the central and southern plateau (Reting, Dasuopu). Although humidity was high according to these archives, the ASM was weak during that time (Anderson et al., 2002; Gupta et al., 2003). Thus, the findings of Reting and Dasuopu reveal an opposite result due to the common sea/land temperature contrast theory of a weak monsoon during cold phases and a strong monsoon during warm periods (Meehl, 1994; Zhang et al., 2008). The sudden moisture decrease since the late 1870s affects the eastern (Lhamcoka), southern (Dasuopu) and central (Reting) parts of the TP. We agree with the conclusions of Xu et al. (2012) who associate the humidity decline to the decrease of the thermal gradient between the tropical and north Indian Ocean, caused by the reduction of the land-ocean temperature difference. However, the reasons for the temperature contrast reduction are not sufficiently clarified. Lau et al. (2006) attributed the humidity reduction to the increase of greenhouse gas and aerosol emissions, while Duan et al. (2000) discovered a relationship to solar activity. The beginning of the humidity decline precedes the onset of Asia's industrialization and therewith massive aerosol emissions. Thus, solar activity and an accompanied temperature increase seems more plausible to regulate the northern hemispheric temperatures and therewith the thermal land-ocean contrast.

**East Tibet
hydroclimate
variability**

J. Wernicke et al.

Title Page

Abstract

Introduction

Conclusions

References

Tables

Figures



Back

Close

Full Screen / Esc

Printer-friendly Version

Interactive Discussion



**East Tibet
hydroclimate
variability**

J. Wernicke et al.

[Title Page](#)[Abstract](#)[Introduction](#)[Conclusions](#)[References](#)[Tables](#)[Figures](#)[Back](#)[Close](#)[Full Screen / Esc](#)[Printer-friendly Version](#)[Interactive Discussion](#)

In comparison to tree-ring sites located further south (e.g. Liu et al., 2013; Shi et al., 2012), the distinct humidity decline is more pronounced on the central and eastern TP. We follow the tree-ring $\delta^{18}\text{O}$ based observation of Sano et al. (2013) who stated that with increasing distance to the moisture source region (Bay of Bengal) a humidity reduction is amplified. In addition, higher altitudes, such as the Dasuopu ice core, are stronger affected by the monsoon weakening than areas at lower altitudes. Interestingly, an opposite trend is reflected in the snow accumulation rates on the northern Plateau (Dunde), where an increasing snow accumulations coincides with the increase of local and north hemispheric temperatures (Mann et al., 1999; Xu et al., 2006a). The contrasting humidity pattern between north and south Tibet is also documented in other climate reconstructions. For instance, tree-ring width based reconstructions for the north-eastern TP of Huang and Zhang (2007), Shao et al. (2005), and Sheppard et al. (2004) have shown a humidity increase since the end of the LIA, whereas Liu et al. (2013), Sano et al. (2011), and Xu et al. (2013) reported a decrease in the local water availability for the southern TP. Findings of positive glacier mass balances of western and northern located regions and negative balances for southern located glaciers confirm our observation (Neckel et al., 2014). A southeast-northwest gradient of glacier accumulation reduction was also described for south-east Tibet (Loibl et al., 2014).

Lhamcoka is located in the supposed intercept zone between the Indian summer monsoon, the East-Asian monsoon and the westerlies (air masses boundaries proposed by Morrill et al., 2003). Thus, we assume that the humidity conditions at the study site are controlled by these planetary circulation systems. Mölg et al. (2014) postulated an overall influence of the westerlies to the entire TP. According to Sano et al. (2013) and Liu et al. (2012), the westerly influence is invalid at least for the southern TP, where a strong El Niño Southern Oscillation (ENSO) influence has been confirmed. Basically, the North Atlantic Oscillation (NAO), ENSO and the ASM are connected by planetary scale feedback mechanisms (Wang et al., 2001). Their interactive complexity regulates the intensity and occurrence of ASM rainfall (Dugam et al., 1997; Garcia

et al., 2000; Yasunari and Seki, 1992). However, profound knowledge of the alternation properties is essential to interpret the humidity properties at Lhamcoka. We suppose that a strong ASM leads to a higher relative humidity due to enhanced convective activity (intensified cloudiness) at the study site. A strong ASM prevails in phases of reduced sea surface temperature in the Niño region 3.4 (Niño 3.4 SST) and thus is negatively correlated to the humidity conditions at the study site. The NAO influence is less straightforward due to its major impact on the north hemispheric climate during winter and spring (DJF/MAM) (Dugam et al., 1997). However, the Niño 3.4 SST is positively associated to the NAO via the Eurasien snow cover and thus evokes an increase (decrease) land-ocean-temperature contrast (Yasunari and Seki, 1992; Hoerling et al., 2001). Accordingly, a low NAO (weak zonal flow) might induce an El Niño like phenomena in the Tropical Pacific (Garcia et al., 2000). Hence, a weak winter NAO is also negatively correlated to the humidity conditions at the sampling site. Although the NAO impact on north hemispheric climate is strongest during winter, the zonal flow has a global impact in all seasons. We associate a strong summer NAO to reduced humidity properties induced by a blocking effect of the moist air masses, originated from the Bay of Bengal and moving northwards (Mischke and Zhang, 2010). Therefore we suppose a negative relationship between relative humidity and summer (July/August) NAO. To clarify the prevailing forces at the Lhamcoka site we conducted running correlation analysis with the monthly resolved NAO and summer Niño 3.4 SST (see Fig. 7). We refer our analysis to the July/August averages from the monthly reconstructed NAO index (Luterbacher et al., 2002). The SST record is composed of station and interpolated data from the International Comprehensive Ocean-Atmosphere Data Set and provides a monthly resolved data set back to 1870 AD (ICADS, downloaded from <http://climexp.knmi.nl/>). The overall relationship between relative humidity and Niño 3.4 SST is weak ($r = -0.06$, $p = 0.46$) while the correlation with NAO is slightly higher, but still weak ($r = -0.16$, $p = 0.07$). The inverse relationship between the impact of NAO (Niño 3.4 SST) to the reconstructed relative humidity was revealed but shows a non-stationary and sign inconsistent linkage (see Fig. 7b). The correla-

**East Tibet
hydroclimate
variability**

J. Wernicke et al.

Title Page

Abstract

Introduction

Conclusions

References

Tables

Figures



Back

Close

Full Screen / Esc

Printer-friendly Version

Interactive Discussion



tions are not effected by El Niño/ La Niña events (yellow/blue bars in Fig. 7). Additionally, the strength of the connection decreases towards the end of the reconstruction and passes only occasionally the significance level. Thus, a superimposing large-scale circulation influence either from NAO nor Niño 3.4 SST can be confirmed. Therefore we consider relative humidity is being more affected by local climate conditions than by planetary circulation patterns. That assumption is proven by spatial correlations of $\delta^{18}\text{O}$ and the sensible heat flux in 2–10 m above the soil surface. We considered the sensible heat flux as a direct expression of vertical air motion representing the strength of convection. Highly significant negative correlations were observed in the vicinity of the sampling site ($r = -0.75$, $p < 0.01$, see Fig. 8). The negative feedback is induced by an increased evapotranspiration which leads to higher relative air humidity and thus an enhanced sensible heat flux. The ascending air reaches the condensation level and provokes convective rain, what consequently causes a rise in relative air humidity and impedes the loss of lighter isotopes (^{16}O) in the tree-ring cellulose (McCarroll and Loader, 2004). As displayed in Fig. 8, the negative relationship is only a regional phenomenon. Moreover, the association to the center of monsoonal moisture transport, the Bay of Bengal, is weak. These are strong evidences for local phenomena superimposing planetary circulation characteristics.

5 Conclusions

We demonstrated that our 800 years long $\delta^{18}\text{O}$ chronology is suitable for a reliable reconstruction of summer relative humidity. Long-term air humidity variations revealed more humid conditions during the termination of the MWP, relatively stable humidity during the LIA and a sudden decrease in summer humidity after the 1870s. The time series displays significant cyclicities of 162, 112, 56 and 12 years. Similar patterns were verified by several proxy archives. Therefore we assume common forces triggering the cyclicities in all archives. The most recent humidity reduction is more pronounced on the central and eastern TP. Moreover, a contrasting trend was found in ice core data

East Tibet hydroclimate variability

J. Wernicke et al.

Title Page

Abstract

Introduction

Conclusions

References

Tables

Figures



Back

Close

Full Screen / Esc

Printer-friendly Version

Interactive Discussion



and tree-ring moisture reconstructions from the northern TP. Thus, we claim an enhanced influence of the westerlies and an attenuation of the ASM since the late 19th century. This hypothesis is occasionally corroborated by a negative teleconnection to the NAO index and an inverse connection to Niño SST 3.4. However, the large-scale influence of planetary circulation systems are unverifiable due to temporally inconsistent correlations. Nevertheless, we found strong but regional confined correlations to the sensible heat flux. Therefore, we concluded that the humidity conditions at Lhamcoka are dominated by local climate rather than large-scale circulation patterns.

Acknowledgements. The authors thank the German Federal Ministry of Education and Research (BMBF) for the financial support. We also thank Roswitha Höfner-Stich for her efficient and precise work at the mass spectrometer.

References

- An, W., Liu, X., Leavitt, S., Xu, G., Zeng, X., Wang, W., Qin, D., and Ren, J.: Relative humidity history on the Batang–Litang Plateau of western China since 1755 reconstructed from tree-ring $\delta^{18}\text{O}$ and δD , *Clim. Dynam.*, 42, 2639–2654, doi:10.1007/s00382-013-1937-z, 2014. 3330
- Anderson, D., Overpeck, J., and Gupta, A.: Increase in the Asian southwest monsoon during the past four centuries, *Science*, 297, 596–599, doi:10.1126/science.1072881, 2002. 3329, 3337
- Berkelhammer, M. and Stott, L.: Secular temperature trends for the southern Rocky Mountains over the last five centuries, *Geophys. Res. Lett.*, 39, 1–6, doi:10.1029/2012GL052447, 2012. 3333
- Böhner, J.: General climatic controls and topoclimatic variations in Central and High Asia, *Boreas*, 35, 279–295, 2006. 3329, 3331
- Bollasina, M., Ming, Y., and Ramaswamy, V.: Anthropogenic aerosols and the weakening of the South Asian summer monsoon, *Science*, 334, 502–505, doi:10.1126/science.1204994, 2011. 3328

East Tibet hydroclimate variability

J. Wernicke et al.

Title Page

Abstract

Introduction

Conclusions

References

Tables

Figures



Back

Close

Full Screen / Esc

Printer-friendly Version

Interactive Discussion



Böttger, T. and Friedrich, M.: A new serial pooling method of shifted tree ring blocks to construct millennia long tree ring isotope chronologies with annual resolution, *Isot. Environ. Health. S.*, 45, 68–80, 2009. 3332

Bräuning, A.: Climate history of the Tibetan Plateau during the last 1000 years derived from a network of Juniper chronologies, *Dendrochronologia*, 19, 127–137, 2001. 3331

Bräuning, A.: Tree-ring evidence of “Little Ice Age” glacier advances in southern Tibet, *Holocene*, 16, 369–380, 2006. 3331, 3332, 3334

Bunn, A.: A dendrochronology program library in R (dplR), *Dendrochronologia*, 26, 115–124, doi:10.1016/j.dendro.2008.01.002, 2008. 3332

Cook, E. and Kairiukstis, L.: *Methods of Dendrochronology*, Kluwer Academic Publishers, Dordrecht, Boston, London, 1990. 3332, 3335

Cook, E., Briffa, K., and Jones, P.: Spatial regression methods in dendroclimatology: a review and comparison of two techniques, *Int. J. Climatol.*, 14, 379–402, 1994. 3335

Cook, E., Anchukaitis, K., Buckley, B., D’Arrigo, R., Jacoby, G., and Wright, W.: Asian monsoon failure and megadrought during the last millennium, *Science*, 328, 486–489, doi:10.1126/science.1185188, 2010. 3329

Duan, K., Wang, N., Li, Y., and Sun, W.: Accumulation in Dasuopu ice core in Qinghai-Tibet Plateau and solar activity, *Chinese Sci. Bull.*, 45, 1038–1042, 2000. 3337

Dugam, S., Kakade, S., and Verma, R.: Interannual and long-term variability in the North Atlantic Oscillation and Indian Summer Monsoon rainfall, *Theor. Appl. Climatol.*, 58, 21–29, 1997. 3338, 3339

García, R., Ribera, P., Gimeno, L., and Hernández, E.: Letter to the editor: Are the North Atlantic Oscillation and the Southern Oscillation related in any time-scale?, *Ann. Geophys.*, 18, 247–251, doi:10.1007/s00585-000-0247-z, 2000. 3338, 3339

Grießinger, J., Bräuning, A., Helle, G., Thomas, A., and Schleser, G.: Late Holocene Asian summer monsoon variability reflected by $\delta^{18}\text{O}$ in tree-rings from Tibetan junipers, *Geophys. Res. Lett.*, 38, 1–5, doi:10.1029/2010GL045988, 2011. 3329, 3336

Gupta, A., Anderson, D., and Overpeck, J.: Abrupt changes in the Asian southwest monsoon during the Holocene and their links to the North Atlantic Ocean, *Nature*, 421, 354–357, 2003. 3337

Hoerling, M., Hurrell, J., and Xu, T.: Tropical origins for recent North Atlantic climate change, *Science*, 292, 90–92, doi:10.1126/science.1058582, 2001. 3339

East Tibet hydroclimate variability

J. Wernicke et al.

Title Page

Abstract

Introduction

Conclusions

References

Tables

Figures



Back

Close

Full Screen / Esc

Printer-friendly Version

Interactive Discussion



Huang, J.-G. and Zhang, Q.-B.: Tree rings and climate for the last 680 years in Wulan area of northeastern Qinghai-Tibetan Plateau, *Climatic Change*, 80, 396–377, doi:10.1007/s10584-006-9135-1, 2007. 3338

Kumar, K., Rajagopalan, B., and Cane, M.: On the weakening relationship between the Indian monsoon and ENSO, *Science*, 284, 2156–2159, doi:10.1126/science.284.5423.2156, 1999. 3329

Lau, K., Kim, M., and Kim, K.: Asian summer monsoon anomalies induced by aerosol direct forcing: the role of the Tibetan Plateau, *Clim. Dynam.*, 26, 855–864, doi:10.1007/s00382-006-0114-z, 2006. 3337

Laumer, W., Andreau, L., Helle, G., Schleser, G., Wieloch, T., and Wissel, H.: A novel approach for the homogenization of cellulose to use micro-amounts for stable isotope analyses, *Rapid Commun. Mass Sp.*, 23, 1934–1940, doi:10.1002/rcm.4105, 2009. 3332

Leavitt, S.: Tree-ring C-H-O isotope variability and sampling, *Sci. Total Environ.*, 408, 5244–5253, 2010. 3331

Liu, X., An, W., Treydte, K., Shao, X., Leavitt, S., Hou, S., Chen, T., Sun, W., and Qin, D.: Tree-ring $\delta^{18}\text{O}$ in southwestern China linked to variations in regional cloud cover and tropical sea surface temperature, *Chem. Geol.*, 291, 104–115, doi:10.1016/j.chemgeo.2011.10.001, 2012. 3330, 3333, 3338

Liu, X., Zeng, X., Leavitt, S., Wang, W., An, W., Xu, G., Sun, W., Wang, Y., Qin, D., and Ren, J.: A 400-year tree-ring $\delta^{18}\text{O}$ chronology for the southeastern Tibetan Plateau: implications for inferring variations of the regional hydroclimate, *Global Planet. Change*, 104, 23–33, doi:10.1016/j.gloplacha.2013.02.005, 2013. 3330, 3333, 3336, 3338, 3354

Liu, X., Xu, G., Griebinger, J., An, W., Wang, W., Zeng, X., Wu, G., and Qin, D.: A shift in cloud cover over the southeastern Tibetan Plateau since 1600: evidence from regional tree-ring $\delta^{18}\text{O}$ and its linkages to tropical oceans, *Quaternary Sci. Rev.*, 88, 55–68, doi:10.1016/j.quascirev.2014.01.009, 2014. 3330, 3335

Loibl, D., Lehmkuhl, F., and Griebinger, J.: Reconstructing glacier retreat since the Little Ice Age in SE Tibet by glacier mapping and equilibrium line altitude calculation, *Geomorphology*, 214, 22–39, doi:10.1016/j.geomorph.2014.03.018, 2014. 3338

Luterbacher, J., Xoplaki, E., Dietrich, D., Jones, P., Davies, T., Portis, D., Gonzalez-Rouco, J., von Storch, H., Gyalistras, D., Casty, C., and Wanner, H.: Extending north atlantic oscillation reconstructions back to 1500, *Atmos. Sci. Lett.*, 2, 114–124, 2002. 3339

East Tibet hydroclimate variability

J. Wernicke et al.

Title Page

Abstract

Introduction

Conclusions

References

Tables

Figures



Back

Close

Full Screen / Esc

Printer-friendly Version

Interactive Discussion



- Mann, M., Bradley, R., and Hughes, M.: Northern Hemisphere temperatures during the past Millennium: inferences, uncertainties, and limitations, *Geophys. Res. Lett.*, 26, 759–762, 1999. 3338
- McCarroll, D. and Loader, N.: Stable isotopes in tree rings, *Quaternary Sci. Rev.*, 23, 771–801, 2004. 3329, 3340
- 5 Meehl, G.: Influence of the land surface in the Asian summer monsoon: external conditions versus internal feedbacks, *J. Climate*, 7, 1033–1049, 1994. 3337
- Mischke, S. and Zhang, C.: Holocene cold events on the Tibetan Plateau, *Global Planet. Change*, 72, 155–163, 2010. 3339
- 10 Mölg, T., Maussion, F., and Scherer, D.: Mid-latitude westerlies as a driver of glacier variability in monsoonal High Asia, *Nature Climate Change*, 4, 68–73, doi:10.1038/NCLIMATE2055, 2014. 3338
- Morrill, C., Overpeck, J., and Cole, J.: A synthesis of abrupt changes in the Asian summer monsoon since the last deglaciation, *Holocene*, 13, 465–476, 2003. 3338
- 15 Neckel, N., Kropáček, J., Bolch, T., and Hochschild, V.: Glacier mass changes on the Tibetan Plateau 2003–2009 derived from ICESat laser altimetry measurements, *Environ. Res. Lett.*, 9, 1–7, doi:10.1088/1748-9326/9/1/014009, 2014. 3338
- Pederson, N., Hessler, A., Baatarbileg, N., Anchukaitis, K., and Di Cosmo, N.: Pluvials, droughts, the Mongol Empire, and modern Mongolia, *P. Natl. Acad. Sci. USA*, 11, 4375–4379, doi:10.1073/pnas.1318677111, 2014. 3336
- 20 Roden, J. and Ehleringer, J.: Hydrogen and oxygen isotope ratios of tree ring cellulose for field-grown riparian trees, *Oecologia*, 123, 481–489, 2000. 3334
- Roden, J., Lin, G., and Ehleringer, J.: A mechanistic model for interpretation of hydrogen and oxygen isotope ratios in tree-ring cellulose, *Geochim. Cosmochim. Ac.*, 64, 21–35, 2000. 3329
- 25 Sano, M., Sheshshayee, M., Managave, S., Ramesh, R., Sukumar, R., and Sweda, T.: Climatic potential of $\delta^{18}\text{O}$ of *Abies spectabilis* from the Nepal Himalaya, *Dendrochronologia*, 28, 93–98, doi:10.1016/j.dendro.2009.05.005, 2010. 3330
- Sano, M., Ramesh, R., Sheshshayee, M., and Sukumar, R.: Increasing aridity over the past 223 years in the Nepal Himalaya inferred from a tree-ring $\delta^{18}\text{O}$ chronology, *Holocene*, 1, 1–9, doi:10.1177/0959683611430338, 2011. 3328, 3330, 3338
- 30

East Tibet hydroclimate variability

J. Wernicke et al.

[Title Page](#)

[Abstract](#)

[Introduction](#)

[Conclusions](#)

[References](#)

[Tables](#)

[Figures](#)



[Back](#)

[Close](#)

[Full Screen / Esc](#)

[Printer-friendly Version](#)

[Interactive Discussion](#)



- Sano, M., Tshering, P., Komori, J., Fujita, K., Xu, C., and Nakatsuka, T.: May–September precipitation in the Bhutan Himalaya since 1743 as reconstructed from tree ring cellulose $\delta^{18}\text{O}$, *J. Geophys. Res.-Atmos.*, 118, 8399–8410, doi:10.1002/jgrd.50664, 2013. 3329, 3330, 3338
- Sauer, M., Aellen, K., and Siegwolf, R.: Correlating $\delta^{13}\text{C}$ and $\delta^{18}\text{O}$ in cellulose of trees, *Plant Cell Environ.*, 20, 1543–1550, 1997. 3329
- Shao, X., Huang, L., Liu, H., Liang, E., Fang, X., and Wang, L.: Reconstruction of precipitation variation from tree rings in recent 1000 years in Delingha, Qinghai, *Sci. China Ser. D*, 48, 939–949, doi:10.1360/03yd0146, 2005. 3336, 3338
- Sheppard, P., Tarasov, P., Graumlich, L., Heussner, K.-U., Wagner, M., Österle, H., and Thompson, L.: Annual precipitation since 515 BC reconstructed from living and fossil juniper growth of northeastern Qinghai Province, China, *Clim. Dynam.*, 23, 869–881, 2004. 3336, 3338, 3354
- Shi, C., Daux, V., Zhang, Q.-B., Risi, C., Hou, S.-G., Stievenard, M., Pierre, M., Li, Z., and Masson-Delmotte, V.: Reconstruction of southeast Tibetan Plateau summer climate using tree ring $\delta^{18}\text{O}$: moisture variability over the past two centuries, *Clim. Past*, 8, 205–213, doi:10.5194/cp-8-205-2012, 2012. 3330, 3338
- Sternberg, L.: Oxygen stable isotope ratios of tree-ring cellulose: the next phase of understanding, *New Phytol.*, 181, 553–562, 2009. 3329
- Sun, Y., Ding, Y., and Dai, A.: Changing links between South Asian summer monsoon circulation and tropospheric land-sea thermal contrasts under a warming scenario, *Geophys. Res. Lett.*, 37, 1–5, 2010. 3329
- Thomas, A. and Herzfeld, U.: REGEOTOP: New climatic data fields for east asia based on localized relief information and geostatistical methods, *Int. J. Climatol.*, 24, 1283–1306, doi:10.1002/joc.1058, 2004. 3329
- Thompson, L., Yao, T., Mosley-Thompson, E., Davis, M., Henderson, K., and Lin, P.-N.: A high-resolution millennial record of the South Asian monsoon from Himalayan ice cores, *Science*, 289, 1916–1919, doi:10.1126/science.289.5486.1916, 2000. 3336, 3354
- Torrence, C. and Compo, G.: A practical guide to wavelet analysis, *B. Am. Meteorol. Soc.*, 1, 61–78, 1998. 3336
- Vuille, M., Werner, M., Bradley, R., and Keimig, F.: Stable isotopes in precipitation in the Asian monsoon region, *J. Geophys. Res.*, 110, 1–15, doi:10.1029/2005JD006022, 2005. 3328

East Tibet hydroclimate variability

J. Wernicke et al.

[Title Page](#)

[Abstract](#)

[Introduction](#)

[Conclusions](#)

[References](#)

[Tables](#)

[Figures](#)



[Back](#)

[Close](#)

[Full Screen / Esc](#)

[Printer-friendly Version](#)

[Interactive Discussion](#)



Wang, B., Wu, R., and Lau, K.-M.: Interannual variability of the Asian summer monsoon: contrasts between the Indian and the Western North Pacific–East Asian monsoons, *J. Climate*, 14, 4073–4089, 2001. 3338

Wang, W., Liu, X., Xu, G., Shao, X., Qin, D., Sun, W., An, W., and Zeng, X.: Moisture variations over the past millennium characterized by Qaidam Basin tree-ring $\delta^{18}\text{O}$, *Chinese Sci. Bull.*, 58, 3956–3961, doi:10.1007/s11434-013-5913-0, 2013. 3330

Wieloch, T., Helle, G., Heinrich, I., Voigt, M., and Schyma, P.: A novel device for batch-wise isolation of α -cellulose from small-amount wholewood samples, *Dendrochronologia*, 29, 115–117, doi:10.1016/j.dendro.2010.08.008, 2011. 3332

Wigley, T., Briffa, K., and Jones, P.: On the Average Value of Correlated Time Series, with Application in Dendroclimatology and Hydrometeorology, *J. Clim. Appl. Meteorol.*, 23, 201–213, 1984. 3332

Xu, C., Sano, M., and Nakatsuka, T.: A 400-year record of hydroclimate variability and local ENSO history in northern Southeast Asia inferred from tree-ring $\delta^{18}\text{O}$, *Palaeogeogr. Palaeoclimatol.*, 286, 588–598, doi:10.1016/j.palaeo.2013.06.025, 2013. 3333, 3338

Xu, H., Ai, L., Tan, L., and An, Z.: Stable isotopes in bulk carbonates and organic matter in recent sediments of Lake Qinghai and their climatic implications, *Chem. Geol.*, 235, 262–275, doi:10.1016/j.chemgeo.2006.07.005, 2006a. 3336, 3338, 3354

Xu, H., Hong, Y., Lin, Q., Zhu, Y., Hong, B., and Jiang, H.: Temperature responses to quasi-100-yr solar variability during the past 6000 years based on $\delta^{18}\text{O}$ of peat cellulose in Hongyuan, eastern Qinghai-Tibet plateau, China, *Palaeogr. Palaeoclimatol.*, 230, 155–164, doi:10.1016/j.palaeo.2005.07.012, 2006b. 3329

Xu, H., Hong, Y., and Hong, B.: Decreasing Asian summer monsoon intensity after 1860 AD in the global warming epoch, *Clim. Dynam.*, 39, 2079–2088, doi:10.1007/s00382-012-1378-0, 2012. 3335, 3336, 3337

Yang, B., Bräuning, A., and Yafeng, S.: Late Holocene temperature fluctuations on the Tibetan Plateau, *Quaternary Sci. Rev.*, 22, 2335–2344, doi:10.1016/S0277-3791(03)00132-X, 2003. 3329

Yang, B., Qin, C., Wang, J., He, M., Melvin, T., Osborn, T., and Briffa, K.: A 3.500-year tree-ring record of annual precipitation on the northeastern Tibetan Plateau, *P. Natl. Acad. Sci. USA*, 111, 2903–2908, doi:10.1073/pnas.1319238111, 2013. 3336

East Tibet hydroclimate variability

J. Wernicke et al.

[Title Page](#)

[Abstract](#)

[Introduction](#)

[Conclusions](#)

[References](#)

[Tables](#)

[Figures](#)



[Back](#)

[Close](#)

[Full Screen / Esc](#)

[Printer-friendly Version](#)

[Interactive Discussion](#)



Yao, T., Duan, K., Xu, B., Wang, N., Guo, X., and Yang, X.: Precipitation record since AD 1600 from ice cores on the central Tibetan Plateau, *Clim. Past*, 4, 175–180, doi:10.5194/cp-4-175-2008, 2008. 3336

Yasunari, T. and Seki, Y.: Role of the Asian monsoon on the interannual variability of the global climate system, *J. Meteorol. Soc. Jpn.*, 70, 177–189, 1992. 3339

Yu, L., Qiufang, C., Weiguo, L., Yinke, Y., Junyan, S., Huiming, S., and Xuxiang, L.: Monsoon precipitation variation recorded by tree-ring $\delta^{18}\text{O}$ in arid Northwest China since AD 1878, *Chem. Geol.*, 252, 56–61, doi:10.1016/j.chemgeo.2008.01.024, 2008. 3330

Zang, C. and Biondi, F.: Dendroclimatic calibration in R: The bootRes package for response and correlation function analysis, *Dendrochronologia*, 31, 68–74, doi:10.1016/j.dendro.2012.08.001, 2012. 3332

Zhang, P., Cheng, H., Edwards, R., Chen, F., Wang, Y., Yang, X., Liu, J., Tan, M., Wang, X., Liu, J., An, C., Dai, Z., Zhou, J., Zhang, D., Jia, J., Jin, L., and Johnson, K.: A test of climate, sun, and culture relationships from an 1810-year chinese cave record, *Science*, 322, 940–942, 2008. 3329, 3336, 3337

Zhao, H. and Moore, G.: Reduction in Himalayan snow accumulation and weakening of the trade winds over the Pacific since the 1840s, *Geophys. Res. Lett.*, 33, 1–5, doi:10.1029/2006GL027339, 2006. 3335

Zhou, T., Zhang, L., and Li, H.: Changes in global land monsoon area and total rainfall accumulation over the last half century, *Geophys. Res. Lett.*, 35, 1–6, doi:10.1029/2008GL034881, 2008. 3329

East Tibet hydroclimate variability

J. Wernicke et al.

Table 1. Verification statistics according to the linear transfer model of $\delta^{18}\text{O}$ and relative humidity within the calibration period 1956–1996 AD.

Sign-test (ST)	0.73 ($p < 0.1$)
Product-moment correlation (PMC)	0.67 ($p < 0.01$)
Product means test (PMT)	3.3 ($p < 0.01$)
Reduction of Error (RE)	0.45
Coefficient of efficiency (CE)	0.45

Title Page

Abstract

Introduction

Conclusions

References

Tables

Figures



Back

Close

Full Screen / Esc

Printer-friendly Version

Interactive Discussion



East Tibet hydroclimate variability

J. Wernicke et al.

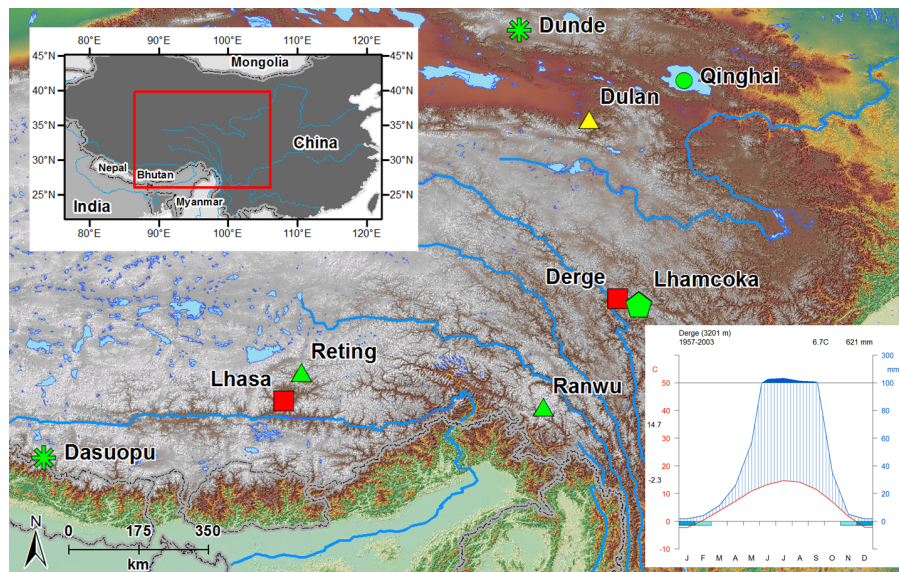


Figure 1. Location of the study site Lhamcoka (green pentagon) and other proxy archives mentioned in the text. Green triangles: tree-ring $\delta^{18}\text{O}$ chronologies; yellow triangle: tree-ring width chronology; green flake: ice cores; green circle: lake sediments. Red rectangles indicate climate stations.

Title Page

Abstract

Introduction

Conclusions

References

Tables

Figures



Back

Close

Full Screen / Esc

Printer-friendly Version

Interactive Discussion



East Tibet
hydroclimate
variability

J. Wernicke et al.

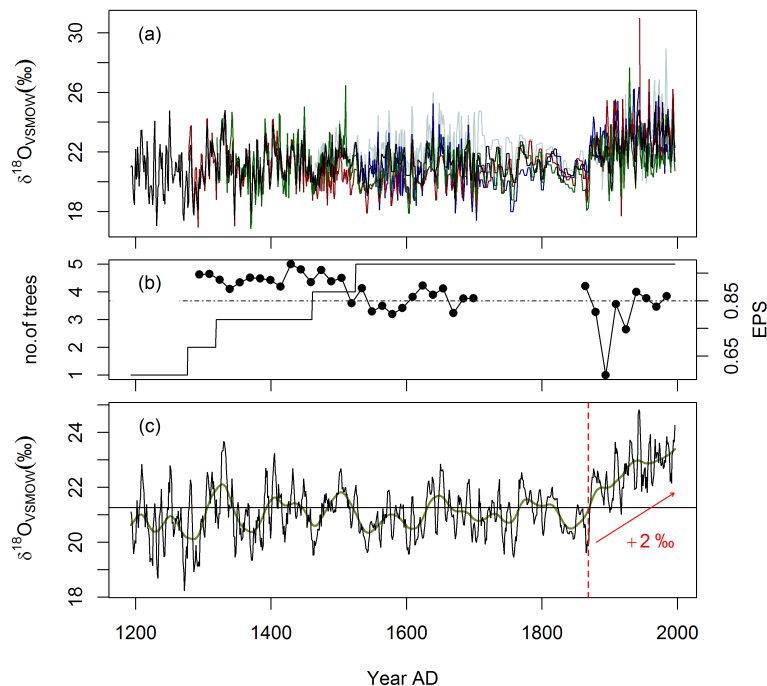


Figure 2. Lhamcoka tree-ring $\delta^{18}\text{O}$ isotope chronology. **(a)** Individual $\delta^{18}\text{O}$ time series of five individuals. The coarse resolution between 1867 and 1707 results from shifted block pooling. **(b)** Running EPS (calculated for 25 year intervals, lagged by 10 years) and number of trees used for the reconstruction (solid line). Dashed line represents the theoretical EPS threshold of 0.85. **(c)** Tree-ring $\delta^{18}\text{O}$ chronology spanning the period 1193–1996 (AD). Green solid line represents a 50 year smoothing spline. Red dashed line marks the turning point towards heavier isotope ratios after ~ 1870 .

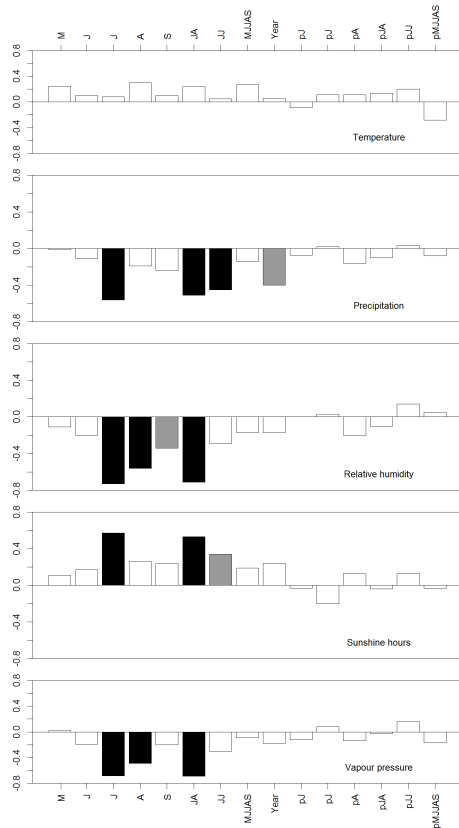


Figure 3. Response of tree-ring $\delta^{18}\text{O}$ to monthly/seasonal temperature, precipitation, relative humidity, sunshine hours and vapour pressure over the period 1956–1996 AD. Gray and black bars indicate correlations significant at $p < 0.05$ and $p < 0.01$; p indicates months/seasons of the previous year.

East Tibet hydroclimate variability

J. Wernicke et al.

Title Page

Abstract Introduction

Conclusions References

Tables Figures

◀ ▶

◀ ▶

Back Close

Full Screen / Esc

Printer-friendly Version

Interactive Discussion



East Tibet hydroclimate variability

J. Wernicke et al.

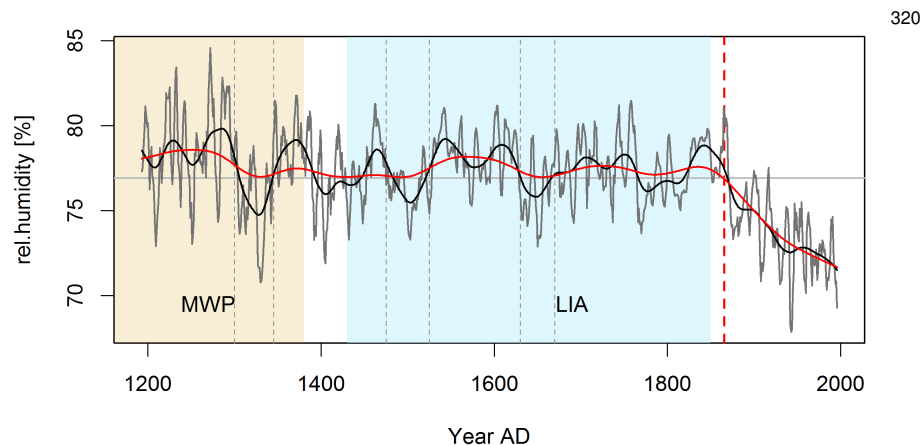


Figure 4. Summer (July and August) relative humidity reconstruction 1193–1996 AD for the eastern TP. Solid black and red lines represent 50 year and 150 year smoothing splines, respectively. Red dashed line emphasises the turning point towards drier conditions (~ 1870 s). The horizontal gray line illustrates mean relative summer humidity ($RH = 72.4\%$). Vertical dashed lines are marking relatively dry periods. The Medieval Warm Period (MWP) and Little Ice Age (LIA) are emphasized in yellow and blue.

Title Page

Abstract

Introduction

Conclusions

References

Tables

Figures



Back

Close

Full Screen / Esc

Printer-friendly Version

Interactive Discussion



East Tibet hydroclimate variability

J. Wernicke et al.

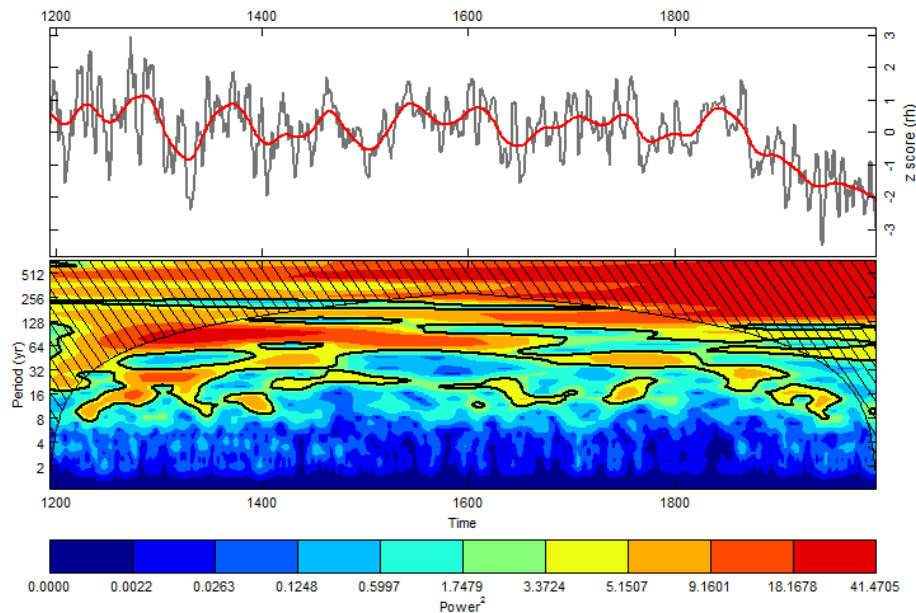


Figure 5. Upper graph shows the standardised summer relative humidity reconstruction smoothed by a 50 years spline curve (red line). Lower panel displays the local wavelet power spectrum of the reconstruction calculated by the Morlet approach. The color code represents the normalized (1/variance) power spectrum of the time series relative to the power spectrum of a white noise process. Black contour is the 95 % significance level. Cone of influence (black shaded) marks regions of the power spectrum influenced by edge effects and therefore have to be excluded from the analysis.

Title Page

Abstract

Introduction

Conclusions

References

Tables

Figures



Back

Close

Full Screen / Esc

Printer-friendly Version

Interactive Discussion



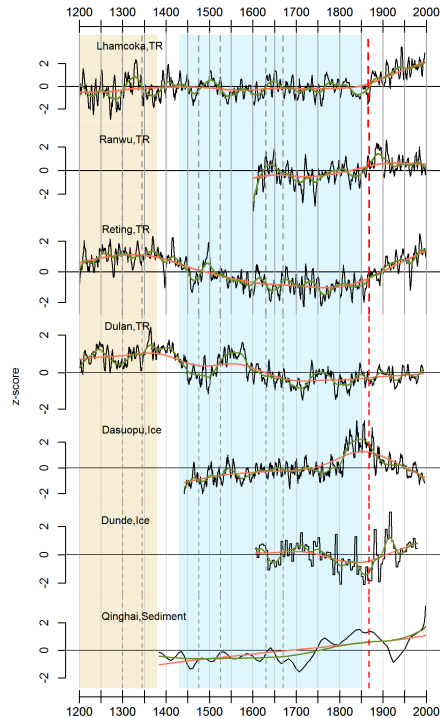


Figure 6. Multiproxy comparison of tree-ring data (TR), ice core and lake sediment data. TR: Lhamcoka this study; Ranwu Liu et al. (2013); Dulan Sheppard et al. (2004). Ice: Dasuopu and Dunde Thompson et al. (2000). Sediment: Qinghai Xu et al. (2006a). Locations of the several proxies are shown in Fig. 1. High positive z-scores indicating dry/warm conditions for TR and sediment records, whereas high z-scores of ice accumulations represents humid conditions, respectively.

East Tibet hydroclimate variability

J. Wernicke et al.

[Title Page](#)

[Abstract](#) [Introduction](#)

[Conclusions](#) [References](#)

[Tables](#) [Figures](#)

[◀](#) [▶](#)

[◀](#) [▶](#)

[Back](#) [Close](#)

[Full Screen / Esc](#)

[Printer-friendly Version](#)

[Interactive Discussion](#)



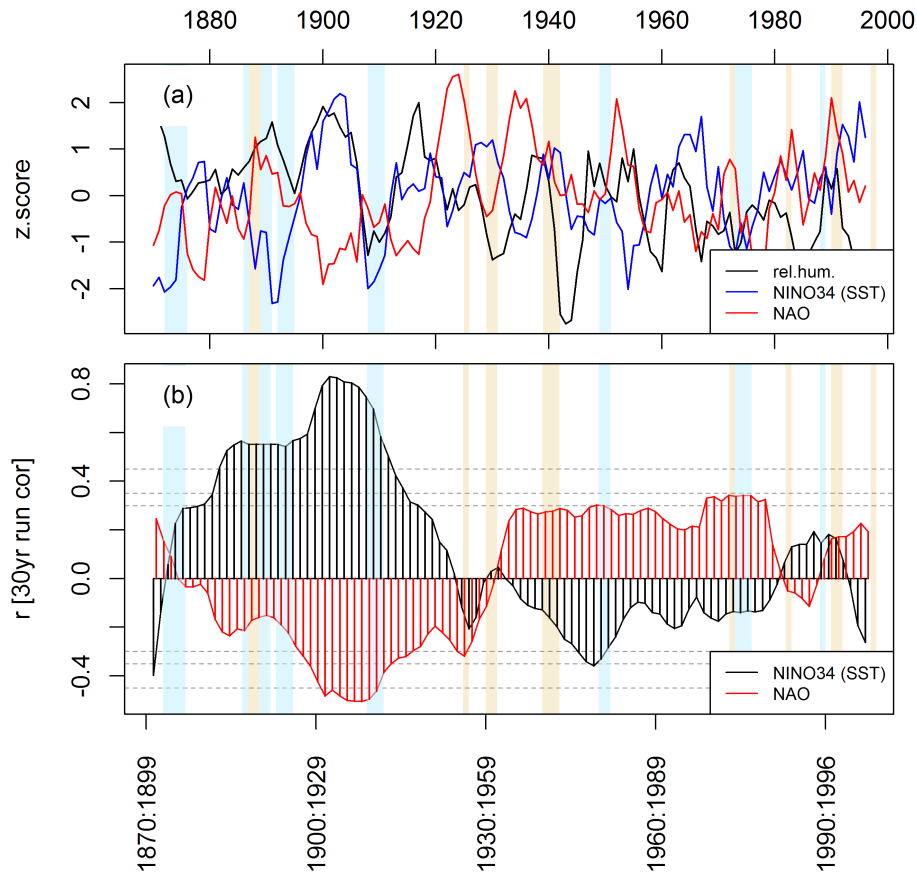


Figure 7. Teleconnection to global circulation pattern: **(a)** 5 years smoothed reconstruction of relative summer humidity (black solid line) compared to the NAO Index for July/August and sea surface temperature of the Niño region 3.4. Phases of strong El Niño/La Niña events are emphasized by yellow/blue bars. **(b)** Running correlation (30 years moving window) between reconstructed relative humidity and SST Niño region 3.4, NAO index July/August, respectively.

Title Page

Abstract

Introduction

Conclusions

References

Tables

Figures



Back

Close

Full Screen / Esc

Printer-friendly Version

Interactive Discussion



East Tibet hydroclimate variability

J. Wernicke et al.

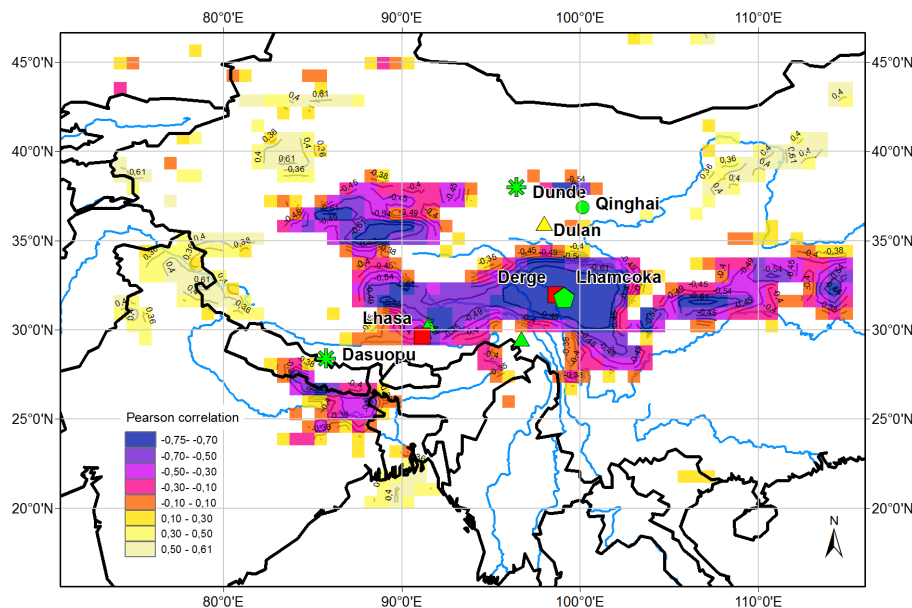


Figure 8. Spatial correlation of $\delta^{18}\text{O}$ and July/August sensible heat flux in 2–10 m above soil surface over the period 1979–1996 AD (ERA interim (European reanalysis data): http://data-portal.ecmwf.int/data/d/interim_daily/). Correlations were calculated by climate explorer (<http://climexp.knmi.nl>) and processed via ArcGIS 10 (ESRI).

Title Page

Abstract

Introduction

Conclusions

References

Tables

Figures



Back

Close

Full Screen / Esc

Printer-friendly Version

Interactive Discussion

